Thickness dependent tortuosity estimation
for retinal blood vessels

Hind Azegrouz, Emanuele Trucco, Baljean Dhillon, Thomas MacGillivray and I.J. MacCormick

Abstract— This paper describes a framework for the automated estimation of vessel tortuosity in retinal images. We introduce a new tortuosity metric that takes into account vessel thickness, yielding estimates plausibly closer to intuition and medical judgement than those from previous metrics. We also propose an algorithm identifying automatically a vasculature segment connecting two points specified manually. Starting from a binary image of the vasculature, the algorithm computes a skeletal (medial axis) representation on which all terminal and branching points are located. This is then converted to a graph representation including connectivity as well as thickness information for all vessels. Target segments for tortuosity estimation are identified automatically from end points selected manually using a shortest-path algorithm. Results are presented and compared with those provided by clinical classification on 50 vessels from DRIVE images. An overall agreement with clinical judgement of 92.4% is achieved, superior to that of comparison measures.

I. INTRODUCTION

The tortuosity of blood vessels in the human retina is a risk indicator linked to many diseases, such as atherosclerosis and hypertension. Tortuosity has been associated with age-related proliferation of blood vessels as well as to degenerative changes of the elastic properties of the vessel walls that allow bending to take place.

To establish a link between tortuosity and vascular pathologies it is desirable to have a quantitative measure of tortuosity, especially within computer-assisted screening programmes. A number of measures have been proposed for image processing [6], [4], [3], [5], but it remains unclear which one is most appropriate. A common one is the *distance metric* [4] defined as the ratio of the vessel length to the chord length between the end points. Other measures proposed are based on curvature of the vessel axis [3], [5] and on direction changes along the vessel [6]. All measures proposed, to our best knowledge, represent blood vessels as one-dimensional curves.

However, the perceived tortuosity of blood vessels seem to depend on thickness as well: in Figure 1, for instance, one would attribute a higher tortuosity level to the thicker

Hind Azegrouz and Emanuele Trucco are with Joint Research Institute Signal and Image Processing, School of Engineering and Physical Sciences, Heriot Watt University, EH14 4AS Riccarton, Scotland, UK {ha19, e.trucco}@hw.ac.uk

Baljean Dhillon is with Princess Alexandra Eye Pavilion, Chalmers Street, Edinburgh, UK, Bal.Dhillon@luht.scot.nhs.uk

Thomas MacGillivray is with The Wellcome Trust Clinical Research Facility, Western General Hospital, Crewe Road, Edinburgh, UK, T.J.MacGillivray@ed.ac.uk

I.J. MacCormick is with The College of Medicine and Veterinary Medicine, University of Edinburgh, The Chancellor's Building 49 Little France Crescent, Edinburgh, UK, s0092761@sms.ed.ac.uk

vessels. Notice that vessel thickness affects also the maximum allowable curvature of the skeleton, which is inversely proportional to thickness (Figure 2, left). In addition, a curve representation does not capture important information related to boundaries (e.g., aneurysms), which is of course captured by thickness analysis (Figure 2, right).

This paper presents a new tortuosity measure using skeleton curvature *as well as* vessel thickness, as opposed to currently used measures [3], [4], [5]. We also propose an algorithm identifying automatically a vasculature segment connecting two points specified manually. Starting from a binary image of the vasculature, the algorithm computes a skeletal (medial axis) representation on which all terminal and branching points are located. This is then converted to a graph representation including connectivity as well as thickness information for all vessels. Target segments for tortuosity estimation are identified automatically given two end points, using a shortest-path algorithm.

The remainder of the paper is organized as follows. Section II sketches the algorithm locating a blood vessel segment between two points selected manually, and Section III gives details. Section IV introduces our tortuosity measure and recalls the standard ones. Section V presents results and compares the tortuosity estimates generated by our system and by a clinician.
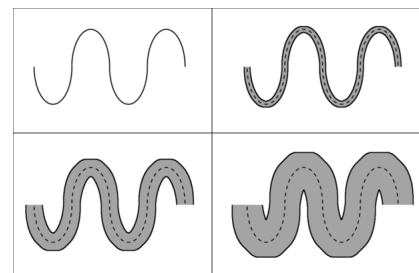

Fig. 1. The larger the thickness, the higher the tortuosity.

II. OUTLINE OF THE ALGORITHM

The algorithm is organized in two stages: (a) location and characterization of a target vessel (Section III), and (b) estimation of vessel tortuosity using the novel metric proposed (Section IV). Figure 3 shows a breakdown of the two stages into modules, discussed in the following sections.

The input is a binary image of the retinal fundus, highlighting the vascular network. A region of interest (ROI)
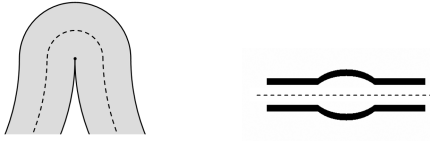
Fig. 2. Left: Thickness limits skeleton bending, i.e., the max curvature achievable. Right: Contour-related features like aneurysms are not captured by skeleton analysis.
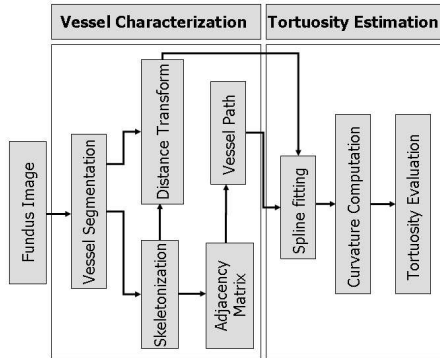

Fig. 3. Outline of the algorithm.

containing the vessels for which tortuosity is to be estimated is selected manually using a GUI. All subsequent operations take place within the ROI.

We first perform binary skeletonisation [7] and compute a graph representation of the vessel network. Crucially, local thickness information are preserved for all arcs using the Euclidean distance transform of the binary image within the ROI. The terminal and branching nodes are then located. Connectivity information obtained so far is organized into an adjacency matrix.

The endpoints of a target vessel, for which tortuosity must be estimated, are then selected by the user via the GUI. Dijkstra's algorithm is applied to find the shortest path between the selected endpoints. The path gives the vessel segment on which tortuosity is estimated.

III. LOCATION AND CHARACTERIZATION OF TARGET VESSELS

A. Skeletonisation

The input image is a binary map of the retinal vasculature. We have used the publicly available DRIVE set by Staal et al. [8]. Figure 4 (top right) shows an example of binary map for the fundus image shown top left. Skeletonisation is performed by the MATLAB *bwmorph* function, based on iterative deletion of pixels and preserving 8-neighbor connectivity. The result for the input image above is shown in Figure 4 (bottom right).

B. Branching and terminal nodes detection

Using the skeleton image, terminal and branching points are detected. We count the number t of transitions from black to white moving clockwise around the 8-neighborhood of a point, which is classified as follows:

- $t=1$: determines a terminal node;
- $t=0, 2$: determines a non-significant point;
- $t \geq 3$: determines a branching point.

Results for the example above are shown in Figure 4 (bottom left).

C. Building the adjacency matrix

We now have the skeleton structure of the vasculature inside the ROI, with arcs associated to portions of detected vessels. Vertex connectivity, i.e., the existence of an arc linking two vertexes, is checked by deleting the vertexes and their 8-neighborhood, then labelling the connected components in the resulting image L; these are the edges of the graph, and a different label is given to each of them. Two vertexes i and j are connected if they lie at the 2 extremities of a constant-label component of L.

We number all the vertexes of the graph and build a connectivity matrix, M_C, in which: $M_C(i,j) = 1$ if vertexes i and j are connected, i.e., belong to the same arc, and $i \neq j$; $M_C(i,j) = \infty$ if i and j are not connected; $M_C(i,j) = 0$ if $i = j$; $M_C(i,j) = M_C(j,i)$, as connectivity is symmetric.

D. Selection of blood vessel segments

A blood vessel segment on which to estimate tortuosity is chosen by selecting two endpoints manually. If there is no branching node between the endpoints, the target segment is given simply by the graph arc containing the two points. Otherwise the segment is given by the shortest path between the endpoints, estimated by Dijkstra's algorithm using the connectivity matrix M_C. Figure 5 shows an example superimposed to the fundus image in Figure 4.

IV. ESTIMATION OF VESSEL TORTUOSITY

A. Boundary localization and curvature estimation

Computing the proposed tortuosity measure for the target segment requires estimates of skeleton curvature and local vessel width.

The set of coordinates of the skeleton pixels on the shortest path, $[X_s(j), Y_s(j)]$, is output by the previous stage and used to estimate curvature; j is a parameter identifying position on the curve, To achieve sensible estimates from the numerical curve, the skeleton is approximated locally by a spline. We used a sampling distance of 3 pixels, which achieves an adequate estimation of tortuosity and limits the effect of sampling noise.

The boundary pixels corresponding to each skeleton point are computed as follows. Let R_s be the vector of the radius (i.e., half-width) values of the vessel cross-section at $[X_s(j), Y_s(j)]$. The corresponding boundary points, $[X_{bi}(j), Y_{bi}(j)]$, $i = 1, 2$, are defined as the intersection of the
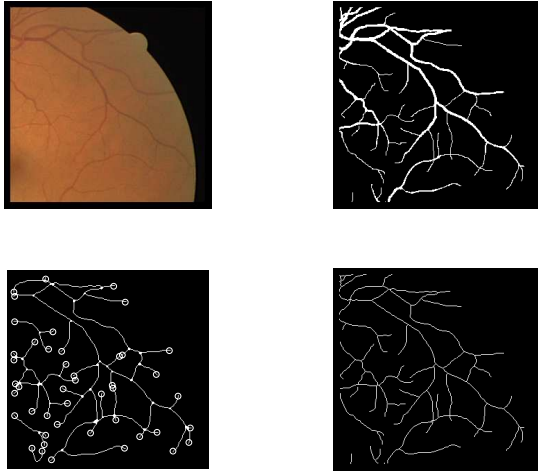
Fig. 4. Top left: fundus image (DRIVE set). Top right: binary image (segmented vasculature). Bottom left: skeleton with branching and endpoints highlighted. Bottom right: extracted skeleton.
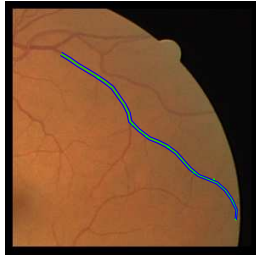

Fig. 5. Vessel segment between manually selected endpoints.

line normal to the skeleton at j and the contours of the vessel in the binary vessel image. Their position is given by (omitting j for simplicity) $X_{bi} = X_s \mp \frac{R_s Y_s'}{\sqrt{X_s'^2 + Y_s'^2}}$ and $Y_{bi} = Y_s \pm \frac{R_s X_s'}{\sqrt{X_s'^2 + Y_s'^2}}$ where the primes indicates differentiation with respect to the curve parameter, j.

B. Comparing tortuosity measures

1) Tortuosity from skeleton only: We use a general measure of tortuosity SCM_p based on local curvature [3], the p-root mean value of curvatures $C_s(j)$. This measure is based only on the skeleton points, $[X_s, Y_s]$.

$C_s(j) = \frac{X_s'(j)Y_s''(j) - X_s''(j)Y_s'(j)}{[X_s'(j)^2 + Y_s'(j)^2]^{3/2}}$

$SCM_p(V) = SCM_p([X_s, Y_s]) = (\sum_j |Cs(j)|^p)^{\frac{1}{p}}$

Where p is a strictly positive integer; we discuss briefly its value below.

2) Tortuosity combining thickness and curvature: We define a tortuosity measure that takes into account the skeleton structure as well the vessels thickness. The intuition is that,

at a parity of skeleton, the curvature of the vessels boundaries (walls) changes with thickness. Our measure, the Absolute p-Curvature Width Metric (CWM_p), is the sum of the averaged curvatures *of pairs of corresponding boundary points*:

$CWM_p(V) = CWM_p([X_s, Y_s], R_s) = (\sum_j \frac{|C_{b1}(j)|^p + |C_{b2}(j)|^p}{2})^{\frac{1}{p}}$.

where C_{b1} and C_{b2} are, respectively, the local curvatures of the two vessel boundary points, $b1$ and $b2$.

This metric has the following properties:

1) $CWM_p([X_s, Y_s], 0) = SCM_p([X_s, Y_s])$: *the measure coincides with the sum-of-curvature metric when the vessel width is zero.*
   Proof: Trivial as in this case the vessel coincides with its skeleton: $CWM_p([X_s, Y_s], 0) = (\sum_j \frac{|C_{b1=s}(j)|^p + |C_{b2=s}(j)|^p}{2})^{\frac{1}{p}}$.

2) $CWM_p([X_s, Y_s], R_s)$ *is an increasing function of R_s.*
   Proof: Without loss of generality we assume a constant radius, $R_s = D$. We first proof that CWM_p increases with D when the skeleton is an arc of a circle of radius R_0, $(D \leq R_0)$, then we generalize to any C^2 curve.
   Let δ be the length of a skeleton arc, and $b1$ and $b2$ the inner and outer boundary points. We have:

   $$C_{b1} = \frac{1}{R_0 - D}, \quad C_{b2} = \frac{1}{R_0 + D}, \quad C_s = \frac{1}{R_0}$$

   Thus, omitting some algebra for brevity,

   $$CWM_p([X_s, Y_s], D) = (\frac{\delta}{2})^{1/p} \frac{R_0}{R_0^2 - D^2} \sum_{2k=0}^{2k<=p} C_p^{2k} (\frac{D}{R_0})^{2k}$$

   which is an increasing function of D. This result generalizes to any C^2 curve considering that, locally, the curve is coincident with an arc of its osculating circle, and applying the proof above to the latter.

3) Increasing p puts more emphasis on high-curvature vessel segments.
   Proof: It follows from the definition of $CWM_p(V)$, where p is a strictly positive integer, that high values of $|C_{b1}(j)|$ and $|C_{b2}(j)|$ contribute with a polynomially increasing term to the tortuosity value.

Figure 6(Left) plots CWM_p for the vessel skeleton in Figure 5, with $p = 1$ and increasing thickness. Notice that CWM_p increases with thickness, as expected (property 2).

V. RESULTS

A. Reference standard

Tests were carried out on ten images of the DRIVE set. On each image, five vessels of interest were highlighted using the algorithm in Section II, for a total of 50 vessel segments spanning different widths, lengths and tortuosity levels. Figure 6 (Right) shows some examples

To establish a standard against which to compare automatic results, the tortuosity of each vessel was assessed by the clinical author (BD), a retinal specialist with experience of diseases causing tortuosity in retinal blood vessels. Three levels were used: not tortuous, low tortuosity, high tortuosity.
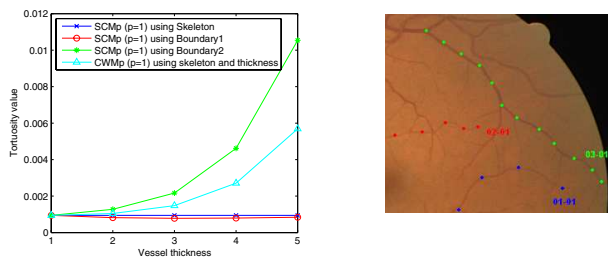
Fig. 6. Left: Plot of SCM_p ($p = 1$) for skeleton and boundaries, and of CWM_p, against increasing thickness (vessel radius) values. The skeleton is that of Figure 5., Right: Zoom on a highlighted DRIVE image.

B. Tests and results

Following [3], we used a logit model [10] which computes a weighted function $x = a + bt_v$, where t_v is the tortuosity of a vessel segment and a, b are weights, then applies the logistic function $h(x) = \frac{\exp(x)}{1 + \exp(x)}$, $h(x) \in [0, 1]$.

A vessel is assigned to one of the three tortuosity classes depending on h: not tortuous if $h \leq 0.33$, low if $0.33 < h < 0.67$, high if $h \geq 0.67$. The weights a and b were optimized on a subset of the vessels [3].

Table I reports percentages of automatic classifications in agreement with clinical judgement. We show results for our measure, with $p = 1$ and $p = 2$, and for the distance metric using only the skeleton [1], [2]. It can be seen that, for this data set, our thickness-dependent measure has an overall better agreement with clinical judgement. Our method achieved a total error rate of 11.2% for $p = 1$ and 7.6% for $p = 2$, giving an overall accuracy of 92.4% for $p = 2$. This compares favorably with the best percentages reported for comparable systems, although of course comparisons in different experimental conditions are only suggestive.

		Clinical Absent	Ground Low	Truthing High
Automatic	Absent	$80, 90, 90$	$18, 8, 10$	$2, 2, 0$
Classification	Low	$6, 2, 19$	$90, 92, 68$	$4, 6, 13$
Results	High	$0, 0, 14$	$6, 4, 26$	$94, 96, 60$

TABLE I

CONFUSION MATRIX OF CLASSIFICATIONS IN PERCENT BETWEEN AUTOMATIC METHOD (ROWS) AND CLINICAL GRADING(COLUMNS) USING CWM_p FOR $p = 1$, CWM_p FOR $p = 2$ AND THE DISTANCE METRIC, RESPECTIVELY.

VI. CONCLUSIONS AND FUTURE WORK

We have presented a new measure for evaluating tortuosity of retinal blood vessels, combining thickness and curvature information. Thickness is considered through its effect on curvatures at vessel boundaries. Initial tests with 50 vessel segments from DRIVE images, of varying thickness, length and tortuosity, suggest that our measure could generate results in better agreement with clinical judgement than based only on vessel skeleton.

Future work will seek to corroborate this conclusion with more extensive data sets and against results of various curvature-based measures. We intend also to identify automatically the optimal value of p via an optimization similar to the one used to determine the logit weights.

Acknowledgement

REFERENCES

[1] N. Patton, T. M. Aslam, T. MacGillivray, I. J. Deary, B. Dhillon, "Retinal image analysis: concepts, applications and potential". *Prog. Retin. Eye Res.* vol. 25 no. 1, pp. 99-127, 2006.

[2] N. Patton, Maini R, T. MacGillivray, T. M. Aslam, I. J. Deary, B. Dhillon B. "Effect of axial length on retinal vascular network geometry." *Amer. Journ. Ophthalmol.* vol. 140 no. 4, pp. 648-53, 2005.

[3] W. Hart and M. Goldbaum and B. Cote and P. Kube and M. Nelson, "Measurement and classification of retinal vascular tortuosity", *Int. Journ. Medical Informatics*, vol. 53, no. 2-3, pp. 239-252, February 1999.

[4] C. Heneghan, J. Flynn, M. OKeefe , M. Cahill, "Characterization of changes in blood vessel width and tortuosity in retinopathy of prematurity using image analysis", *in Medical Image Analysis*, Vol. 6, Issue 4, pp.407-429, Dec 2002.

[5] E. Grisan, M. Foracchia, A. Ruggeri, "A novel method for the automatic evaluation of retinal vessel tortuosity", Proc. 25th IEEE EMBS, pp. 866-869, Sep 2003.

[6] E. Bullitt, G. Gerig, S. Pizer, W. Lin and S. Aylward,"Measuring Tortuosity of the Intracerebral Vasculature from MRA Images", *IEEE Trans. Med. Img.*, vol.22, pp.1163-1171, 2003.

[7] L Lam, S W Lee, C Suen, "Thinning Methodologies: a Comprehensive Survey", *IEEE Trans. Patt. Anal. and Machine Intelligence*, vol. 14, pp. 879 - 884, 1992.

[8] J J Staal, M D Abramoff, M Niemeijer, M A Viergever, B van Ginneken, "Ridge based vessel segmentation in color images of the retina", *IEEE Trans. Medical Imaging*, vol. 23, pp. 501-509, 2004.

[9] O Smedby, N Hogman, S Nilsson, U Erikson, A G Olson , G Walldius, "Two dimensional tortuosity of the superficial femoral artery in early atherosclerosis", *J Vascular Res.*, vol. 30, pp. 181-191,1993.

[10] J Cramer, "The Logit Model: An Introduction for Economics", J Edward Arnold, 1991.